P H Y S I C A L R E V I E W L E T T E R S

Tunable Nonlinear Viscoelastic "Focusing" in a Microfluidic Device

A. M. Leshansky,[1,*] A. Bransky,[2] N. Korin,[2] and U. Dinnar[2]

[1]*Department of Chemical Engineering, Technion-IIT, Haifa, 32000, Israel*
[2]*Department of Biomedical Engineering, Technion-IIT, Haifa, 32000, Israel*
(Received 6 February 2007; published 7 June 2007)

In this Letter we describe a novel method for tunable viscoelastic focusing of particles flowing in a microchannel. It is proposed that some elasticity, inherently present in dilute polymer solutions, may be responsible for highly nonuniform spatial distribution of flowing particles across the channel cross section, yielding their "focusing" in the midplane of the channel. A theory based on scaling arguments is presented to explain the lateral migration and is found to be in a very good agreement with the experimental observations. It was found that, in agreement with the theoretical prediction, the particles would have different spatial distribution depending on their size and rheology of the suspending medium. We demonstrate how the viscoelastic focusing can be precisely controlled by proper rheological design of the carrier solution.

The dynamics and flow of liquids through microfluidic channels are at the heart of numerous proposed technologies. Many such applications require manipulation (e.g., focusing, sorting, etc.) of flowing particles or biological cells. For example, in flow cytometry cells or particles are spatially focused using core-sheath flows to facilitate their detection by laser scattering or fluorescence emission [1]. Flow cytometry is used in a wide variety of applications including hematology [2], bacterial analysis [3], and particle-based assays [4], and there is an enormous interest in miniaturizing these systems. Since micromachined flow cells are restricted to planar structures, the focusing methods used in conventional flow cytometry are not applicable and other techniques for in-flow manipulation were developed, such as dielectrophoretic [5], acoustic [6], and electokinetic focusing [7]. However, there is no simple and robust microfluidic technology for passive manipulation that does not require complex geometry, sheath flows or application of external fields.

Over the years, there was a considerable amount of work on lateral flow-induced migration of particles in unidirectional laminar flows, and several mechanisms have been identified and studied. In the absence of appreciable inertial effects, the governing equations of motion are linear and invariant under a reversal of the velocity; thus rigid spherical particles (or symmetric nonspherical particles undergoing continuous "flipping") suspended in a tube or channel flow cannot migrate laterally [8]. The cross-stream particle migration may be attributed to either non-negligible inertial forces [9], particle (such as erythrocyte) deformability [10], shear-induced diffusion due to multiparticle chaotic hydrodynamic interactions [11], or non-Newtonian effects [12,13].

In this Letter, we report a methodology for passive and tunable focusing of particles or cells in dilute suspensions in a flow-through geometry. The results of the microfluidic experiments demonstrate how the intrinsic nonlinear elas-

tic forces arising in pressure-driven flows of dilute polymer solutions can be exploited to drive particles away from walls, towards the midplane of the channel in a controllable fashion. We present results of the analytical model to describe the underlying migration mechanism and propose ways for fine-tuning of the transverse particle distribution. Lastly, results of experiments, designed to verify the theoretical predictions, are provided and thoroughly discussed.

In our experiments, we use shallow microfluidic channels of a cross section $h \times w = 45 \times 10^3 \ \mu m^2$ fabricated in microscope cover glasses using photolithography as described previously [14]. A syringe pump (KDS 210, KD Scientific) was used to infuse a dilute (< 0.1 vol.%) monodisperse suspension of polystyrene (PS) microspheres (Duke Scientific) through a microchannel inlet at various constant flow rates (the typical velocities of 0.1–1 cm/s). A high speed CCD camera (CPL MS1000 Canadian Photonic Labs) was mounted on an upright microscope (Nikon 80i). Films of microspheres flowing at the center of the microchannel (at the distance $w/2$ from the side walls) 20 mm downstream from the inlet at various depths, were recorded directly on a PC, for further analysis by a custom designed image-processing software [14]. The algorithm is capable of counting particles and calculating their velocity in a thin vertical layer of $\sim 1 \ \mu m$ depth.

We define the particle distribution function (PDF) as the fraction of particles registered in focus at a certain depth, divided by their streamwise velocity and normalized to unity. According to this definition, the PDF must be constant and flow-rate independent, provided that particles follow the streamlines of the ambient flow. We first perform a reference experiment with 8-μm diameter PS microspheres suspended in a viscous Newtonian liquid containing 84 vol % glycerol in deionized water. The solution shear viscosity was measured using a strain-controlled rheometer (ARES, Rheometric Scientific) and was found to be ~ 0.063 Pa s at 25 °C. Figure 1(a) repre-
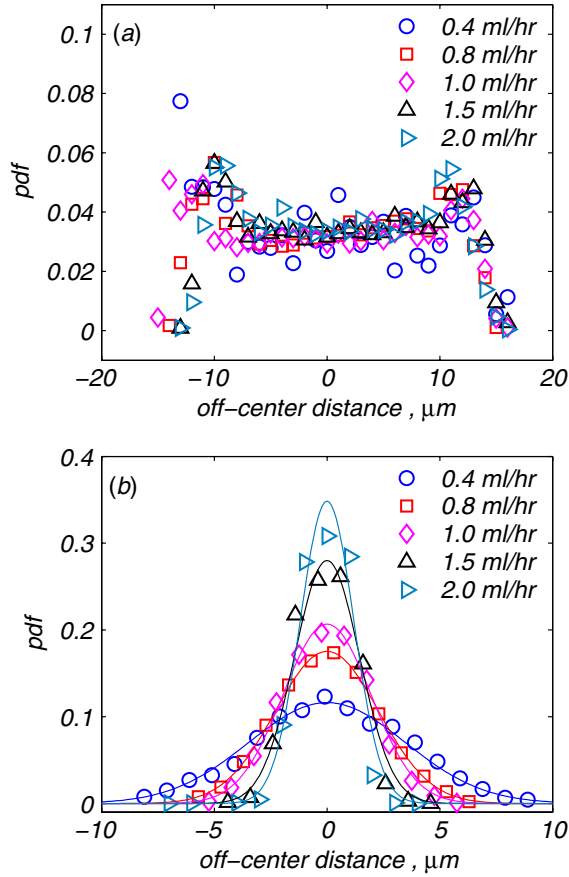
FIG. 1 (color online). The PDF of the 8 μm-diameter PS microspheres vs the vertical off-center distance. The void symbols are the experimental results. (a) glycerol solution, (b) PVP solution. The solid lines are the Gaussian fits to the experimental data.

sents the experimental PDF vs the off-center vertical distance upon varying the flow rate. Each point corresponds to a mean value based on hundreds of individual measurements. It is readily seen that particle distribution does not vary with the flow rate and is mostly uniform [15]. We repeat the experiment with PS microspheres suspended in 8 wt % polyvinylpyrrolidone (PVP, $M_W \approx 3.6 \times 10^5$; Sigma-Aldrich) water solution and plot the resulting PDF in Fig. 1(b). It is readily seen, that the particles tend to migrate away from the walls and concentrate in the midplane, while the focusing intensifies with an increase in flow rate. Obviously, the deformation-induced migration is not operative for rigid microspheres; inertial effects should yield similar results in both solutions, while shear-induced migration is only observed in concentrated suspensions.

We shall next demonstrate that the lateral particle migration is driven by the imbalance of the compressive nonlinear elastic forces. These forces in shearing flows are described in terms of the 1st and 2nd normal stress differences, $N_1(\dot{\gamma}) = \sigma_{xx} - \sigma_{yy}$ and $N_2(\dot{\gamma}) = \sigma_{yy} - \sigma_{zz}$, respectively [16] (here σ_{ii} stands for the diagonal component of the stress tensor, x denotes the direction of the flow,

y is the direction of velocity gradient, and z is the vorticity direction). The rigorous analysis of lateral particle migration in plane Poiseuille flow for an analytically tractable case of second-order viscoelastic fluid showed that both $N_1 > 0$, $N_2 < 0$ act to drive particles towards the center of the channel [13]. In order to keep the analysis as general as possible, we construct a simple theory based on scaling arguments. We neglect the N_2 contribution [17] and assume the transverse elastic force exerted on the particle is proportional to the variation of N_1 over the size of the particle, $F_e \sim a^3(\partial N_1(\dot{\gamma})/\partial y)$ and counterbalanced by the Stokes drag, $F_\eta = 6\pi\eta(\dot{\gamma})aV$. Here V is the velocity of lateral migration, a is the radius of the particle, $-d \leq y \leq d$, d is the half-depth of the channel, η is the dynamic viscosity that is in general a function of the local shear rate $\dot{\gamma}$. Equating F_e and F_η yields the expression for the lateral migration speed

$$V \sim -\frac{a^2}{6\pi\eta}\frac{\partial N_1}{\partial \dot{\gamma}}\frac{\partial \dot{\gamma}}{\partial y}. \tag{1}$$

For the aspect ratio of $w/h \approx 22$ we approximate the flow by the plane Poiseuille profile. For the power-law fluid, $\eta = m\dot{\gamma}^{n-1}$ with $\dot{\gamma} = |du/dy|$ the solution is given by $u(y) = \frac{1+2n}{1+n}\bar{U}[1-(\frac{y}{d})^{1+1/n}]$, where $\bar{U}$ is the mean velocity. A power-law behavior, $N_1 = A\dot{\gamma}^\beta$ $(1 < \beta \leq 2)$, is expected for dilute solutions of high molecular weight polymers [16]. Thus, substituting N_1 and $\dot{\gamma}$ into (1) we arrive at

$$V = \mathcal{C}\alpha\bar{U}^\alpha|\zeta|^{\lambda-n/n}, \tag{2}$$

where $\alpha = \frac{a^2\beta A}{6\pi mnd}(\frac{1+2n}{nd})^\lambda$ has the dimensions of $[L/T]^{1-\beta}$, $\lambda = 1 + \beta - n$ and $\zeta = y/d$ is the scaled transverse coordinate and $\mathcal{C}$ is a constant to be determined later by fitting the model to the experimental data.

We further neglect Brownian forces, the hydrodynamic interaction among particles and with the walls, and assume that the streamwise velocity U of the particle is approximately equal to the velocity of the undisturbed flow, u, at its center [18]. Therefore, the trajectory of the particle is the solution of the following equation

$$\frac{d\zeta}{d\xi} = \frac{V}{U} = -\frac{1+n}{1+2n}\frac{\mathcal{C}\alpha\bar{U}^{\lambda-1}|\zeta|^{\lambda-n/n}}{1-\zeta^{n+1/n}}, \tag{3}$$

where $\xi = x/d$ is the scaled axial coordinate. Equation (3) can be readily integrated and the implicit solution of the form $\mathcal{F}(\zeta, \zeta_0) = \mathcal{C}\alpha\bar{U}^{\lambda-1}\xi$ can be obtained. Assuming that initially the particle distribution across the channel cross section is uniform, we can estimate the half-width of the central core containing 95% of the particles, y_{95}, at the distance ξ from the entrance due to "viscoelastic focusing." Since the envelope of the core is a trajectory, we can compare the experimental results in Fig. 1(b) with the theoretical model based on the solution of (3). The shear viscosity of the PVP solution measured with the ARES rheometer at 25 °C and is found equal to ~0.064 Pa s. The observed shear-thinning was minor as the viscosity dimin-

ishes by less than 3% over the range of shear rates of
0.1–250 s^{-1} (see the inset in Fig. 2) and, therefore, we
use $n = 1$ for the PVP solution.

The magnitude of N_1 for the PVP solution was too low to
be reliably measured in steady shear tests. Instead, we per-
formed the small-amplitude oscillatory shear measure-
ments of the dynamic rigidity (''storage modulus''), G',
as a function of the oscillation frequency, ω (see Fig. 2).
Using the rheometric relationship $G'(\omega)/\omega^2 \sim$
$N_1(\dot{\gamma})/2\dot{\gamma}^2$, that holds between G' and N_1 at low values
of $\dot{\gamma}$ and ω, we can estimate the value of $N_1 \simeq$
$0.94\dot{\gamma}^{1.54}$ mPa. The analogous Cox-Merz relation holds
between the shear viscosity $\eta(\dot{\gamma})$ and the absolute value
of the complex viscosity $|\eta^*(\omega)|$, as confirmed in the inset
in Fig. 2.

Given the rheological properties and the channel dimen-
sions we can calculate α directly and then find the multi-
plication constant $\mathcal{C}$ by fitting the solution of (3) to the
experimental data. The values corresponding to $y_{95}(\mu m)$
are calculated from the data shown in Fig. 1 for various
flow rates and presented in Fig. 3 as open triangles. The
(blue, middle) curve in Fig. 3 corresponds to the best fit of
the theoretical model to the experimental data and there is
an excellent agreement between the two. The best fit yields
the multiplication constant $\mathcal{C} \approx 0.301$.

The scaled width of the PDF due to Brownian forces in a
steady state, $2\zeta_B$, can be estimated from the condition Pe $=$
$aV/D_0 = 1$, where V is given by (2), D_0 is the Stokes-
Einstein diffusivity of a single particle, and Pe is the Péclet
number. For $a = 0.5$ μm and $\bar{U} = 1$ cm/s one obtains
$\zeta_B \approx 0.004$, so the Brownian transport can be entirely
neglected for μm-size particles.

The expression (2) yields $V/\bar{U} \sim \alpha\bar{U}^{\beta-n}$, where the
strength of the focusing is controlled by $\alpha \sim Aa^2/\eta$. The
shear thinning (i.e., $n < 1$) may reinforce the focusing.
The ratio of depth-averaged migration velocities of shear

thinning and Newtonian liquids (with the same elastic
properties and zero-shear-rate viscosity) reduces to
$(\frac{1+2n}{n}\frac{\bar{U}}{d})^{1-n}$ s^{1-n}, and for $\bar{U}/d > 1$ s^{-1} this expression is
larger than 1 for $n < 1$. Thus, by varying the particle size
and altering the elasticity and/or viscosity of the suspend-
ing medium one can control the width of the particle
distribution at a certain distance downstream. For instance,
if the N_1 exponent $\lambda \approx 1$, the particle distribution is ex-
pected to be insensitive to the flow rate. To verify the
validity of the theoretical prediction, we repeat the ex-
periments using the viscoelastic liquid based on dilute
solution of high molecular weight polyacrylamide (PAA),
prepared using a solvent of 76 wt % glycerol with 45 ppm
PAA (Separan AP30; Dow Chemical Co.). The shear vis-
cosity varies from 0.052 to 0.036 Pa s over the range of
shear rates 0.1–450 s^{-1} and is best approximated by $\eta \simeq$
$0.047\dot{\gamma}^{-0.06}$ Pa s (see the inset in Fig. 2). The dynamic
rigidity measurements yield $N_1 \approx 0.0116\dot{\gamma}^{1.09}$ Pa (see
Fig. 2).

Thus, $V/\bar{U} \sim \bar{U}^{0.15}$, and rather weak dependence of the
PDF on the flow rate is anticipated. On the other hand, the
preexponential factor A is about an order of magnitude
higher than that measured for the PVP solution, and, there-
fore, a stronger focusing effect is expected in the PAA
solution.

The resultant PDF of the 8 and 5 μm microspheres are
given in Figs. 4(a) and 4(b), respectively. It can be readily
seen that the PDF is almost independent of the flow rate as
expected. Also, the particle size effect is evident: the PDF
distribution is narrower for larger particles. The corre-
sponding values of y_{95} can be calculated from the PDF's
in Fig. 4 and they are depicted in Fig. 3 vs the flow rate for
the 5 (open diamond) and 8 μm particles (open square).
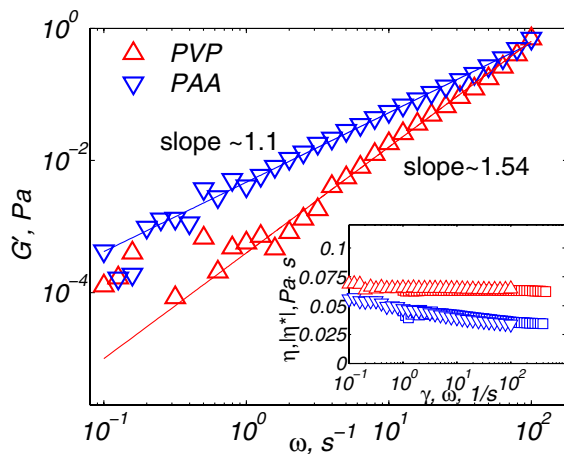The theoretical prediction of y_{95} in the PAA solution [black

FIG. 2 (color online).   The rigidity modulus, G', of the polymer
solutions vs the oscillatory frequency ω (log-log plot). The inset
shows the shear viscosity, η ($\square$), and the complex viscosity, $|\eta^*|$
($\triangle$, $\triangledown$), of polymer solutions vs $\dot{\gamma}$ and ω, respectively.
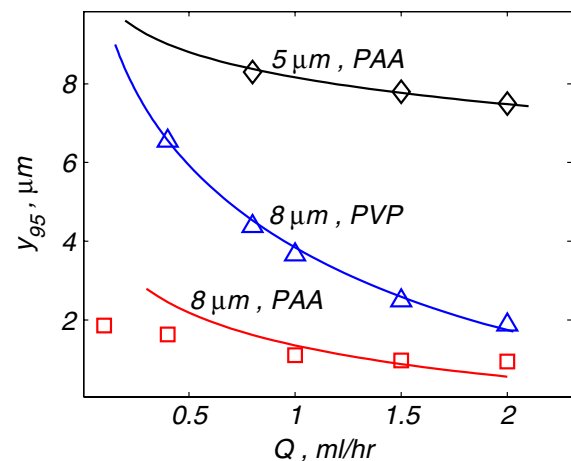

FIG. 3 (color online).   Comparison between the experimental
results (void symbols) and the theoretical prediction (solid
curves): 8 μm particles, the PVP solution ($\triangle$); 8 μm particles,
PAA solution ($\square$); 5 μm particles, PAA solution ($\diamond$). The
theoretical curves corresponding to PAA solution have no ad-
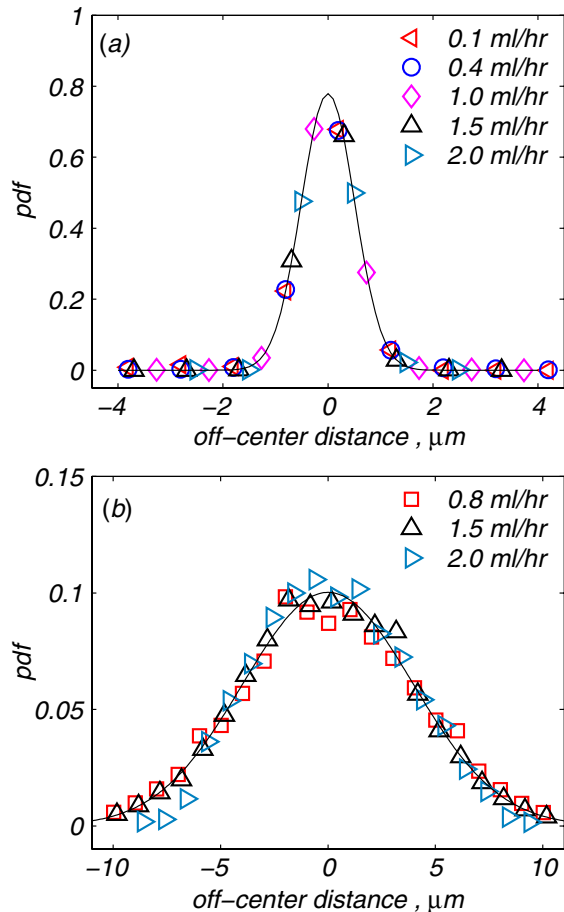justable parameter.

FIG. 4 (color online). The PDF of the PS microspheres suspended in the PAA solution vs the vertical off-center position. The void symbols are the experimental results. (a) 8 μm-diameter particles; (b) 5 μm-diameter particles. The solid lines serve to guide the eyes.

(top) and red (bottom) curves in Fig. 3] is based on the solution of (3) with $\mathcal{C} = 0.301$ and does not involve any adjustable parameters. As expected, the focusing effect for 8 μm particles is stronger in the PAA solution than in the PVP solution and the effect of the particle size is considerable. The comparison between the theoretical estimate (without adjustable parameters) and the experimental data shows excellent agreement and validates the hypothesis of the viscoelastic focusing. The agreement between the theoretical prediction and the experiment for 8 μm particles in PAA solution in Fig. 3 is less accurate than that for 5 μm particles, as the experimental resolution in the former case is insufficient: the particles are focused in a very thin layer [<4 μm, see Fig. 4(a)].

To conclude, we showed that in a microfluidic format very small normal elastic forces (often inherently present) may result in a highly nonuniform transverse particle distribution. We further developed a simple theory and proposed ways for fine-tuning of passive focusing via proper rheological "design" of the carrier solution. Ex-

periments with extradilute PAA solutions confirm the theoretical prediction and exhibit robust focusing with particle distribution being insensitive to variation in the flow rate. The prediction of the theoretical model is in excellent quantitative agreement with the experimental data. The quadratic dependence of the migration speed on the particle size can be potentially used for sorting of biological cells in a flow-through geometry. In particular, viscoelastic focusing is expected to considerably facilitate size segregation in hydrodynamic chromatography [19].

*Electronic address: lisha@tx.technion.ac.il

[1] V. Kachel, H. Fellner-Feldegg, and E. Menke, *Flow Cytometry and Sorting* (Wiley, New York, 1990).

[2] M. Brown and C. Wittwer, Clin. Chem. **46**, 1221 (2000); S. F. Kingsmore, Nat. Rev. Drug Discov. **5**, 310 (2006).

[3] P. P. Fouchet *et al.*, Biol. Cell **78**, 95 (1993).

[4] J. S. Klutts *et al.*, J. Clin. Microbiol. **42**, 4996 (2004); O. Shovman *et al.*, Ann. N.Y. Acad. Sci. **1050**, 380 (2005).

[5] D. Holmes, H. Morgan, and N. G. Green, Biosens. Bioelectron. **21**, 1621 (2006).

[6] G. Goddard *et al.*, Cytometry **69**, 66 (2006).

[7] D. P. Schrum *et al.*, Anal. Chem. **71**, 4173 (1999).

[8] R. G. Cox and S. G. Mason, Annu. Rev. Fluid Mech. **3**, 291 (1971).

[9] G. Segré and A. Silberberg, J. Fluid Mech. **14**, 136 (1962); P. B. P. Ho and L. G. Leal, J. Fluid Mech. **65**, 365 (1974); J. A. Schonberg and E. J. Hinch, J. Fluid Mech. **203**, 517 (1989).

[10] H. L. Goldsmith, Federation Proceedings **30**, 1578 (1971); H. L. Goldsmith and S. G. Mason, J. Colloid Interface Sci. **17**, 448 (1962); P. Olla, Phys. Rev. Lett. **82**, 453 (1999).

[11] D. Leighton and A. Acrivos, J. Fluid Mech. **181**, 415 (1987); R. J. Phillips *et al.*, Phys. Fluids A **4**, 30 (1992); D. J. Pine *et al.*, Nature (London) **438**, 997 (2005).

[12] K. Karnis and S. G. Mason, Trans. Soc. Rheol. **10**, 571 (1966); F. Gauthier, H. L. Goldsmith, and S. G. Mason, Trans. Soc. Rheol. **15**, 297 (1971); M. A. Tehrani, J. Rheol. (N.Y.) **40**, 1057 (1996); P. Y. Huang *et al.*, J. Fluid Mech. **343**, 73 (1997).

[13] B. P. Ho and L. G. Leal, J. Fluid Mech. **76**, 783 (1976).

[14] A. Bransky *et al.*, Biosens. Bioelectron. **22**, 165 (2006); Microvasc. Res. **73**, 7 (2007).

[15] The particle Reynolds number $\mathrm{Re}_p = \mathrm{Re}(a/h)^2 \simeq 5 \times 10^{-5}$ is too small for inertial lift forces [9] to be responsible for the particle-free depletion layer near the walls observed in Fig. 1, while it is probably of a non-hydrodynamic origin (e.g., electrostatic repulsion).

[16] H. A. Barnes, J. F. Hutton, and K. Walters, *An Introduction to Rheology* (Elsevier, Amsterdam, 1989).

[17] For most polymeric systems the ratio $|N_2|/N_1 < 0.1$ [16].

[18] In Poiseuille flow of the Newtonian liquid the mismatch between the particle velocity and the velocity of the ambient flow, i.e., the "slip" velocity $\sim \bar{U}(a/d)^2$.

[19] J. A. Davis *et al.*, Proc. Natl. Acad. Sci. U.S.A. **103**, 14 779 (2006).